# Numerical Simulation of Two-Phase Flow field and Performance Prediction for Solid Rocket Motor Nozzle

*Shafqat Wahab[1], Xie Kan[2]*
*[1,2]PhD candidate, School of Astronautics*
*Beijing University of Aeronautics & Astronautics, (BUAA), China*
*shafqatwahab99@yahoo.com*

*Liu Yu*
*Professor School of Astronautics*
*Beijing University of Aeronautics & Astronautics, (BUAA), China*
*37 Xue Yuan, Road, Beijing 100083, China*

*Key Words: Solid Rocket Motor, Nozzle Geometry, Two Phase Flow Field, Performance Optimization*

## Abstract

This paper presents numerical investigation of multi-phase flow in solid rocket motor nozzle and effect of multi-phases on the performance prediction of the Solid Rocket Motor. Aluminized propellants are frequently used in solid rocket motors to increase specific impulse. An Eulerian-Lagrangian description has been used to analyze the motion of the micrometer sized and discrete phase that consist of the larger particulates present in the Solid Rocket Motor. Uniform particles diameters and Rosin-Rammler diameter distribution method has been used for the simulation of different burning of aluminum droplets generating aluminum oxide smokes. Roe-FDS scheme has been used to simulate the effects of the multi-phase flow. The results obtained show the sensitivity of this distribution to the nozzle flow dynamics, primarily at the nozzle inlet and exit. The analysis also provides effect of two phases on performance prediction of Solid Rocket Motor.

## Introduction

The aluminum powders are used in solid rocket motor propellant for the purpose of increasing the motor specific impulse. As the aluminum burns with high temperature without any adverse effects on the detonation characteristics of the propellant, but it significantly affects the flow field of the chamber and nozzle. Several different metals have been considered and used in solid propellants with aluminum being extensively used in mass fractions of 12-22 %[1)]. High density and high heat of reaction are two factors which contribute to high impulse. It is known that the flow field of the solid rocket motor is very complicated due to the chemical reaction, particle evaporation, combustion, and break up and other complex characteristics like agglomeration and coalescence etc. So these effects cause nozzle erosion and significant exhaust products. Therefore aluminum behavior is one of the most important challenges faced by the solid propellant rocket industry[2)].

During the combustion of aluminized propellant, the aluminum particles in the propellant melt and form liquid aluminum at the burning propellant surface. Because of the physical properties of aluminum and its oxide, a large fraction of aluminum remains un-reacted and in liquid state at the burning propellant surface. Several liquid droplets merge into large agglomerates[1)]. These agglomerates leave the propellant surface and continue to burn relatively slowly due to low volatility of aluminum. The vaporized aluminum reacts with the oxidizing species in the gas phase forming aluminum oxide. Whereas most of this aluminum oxide “smoke” diffuses outward into the flow field, a part is captured on the agglomerate surface and condenses to form an oxide shell. The formation of aluminum oxide shell on the surface of the droplet further contributes to the “slowness” of aluminum combustion.

Therefore the flow within the rocket is multiphase or two phase, because it contains droplets and smoke particles. The two phase flow representing bimodal distribution of aluminum oxide representing the smoke and the caps, which are on the order 1.5 and 100 μm in size respectively. Several Combustion scientists and propulsion engineers have conducted many studied aimed at determining the size distribution of the $Al_2O_3$ droplets present in the motor, nozzle and exhaust plume, because of the large effect on the impulse efficiency. So this area still required a lot of attentions on the size distributions of the droplets entering the chamber and nozzle. Sabnis et al[3)] refer to Salita’s[4)] quench-bomb investigations, where the size distribution was found to be lognormal and bimodal. Typical values of the weighted mean diameters were 1.5μm for the small particles; where as the larger particles were 150 μm with the standard deviation of 0.2. However Whitesides et al[5)] analyzed a reusable solid rocket production propellant, and concluded that a single lognormal or polynomial distribution did not adequately fit the measured droplet diameter distribution. So such contradictory conclusion indicates that the droplet size distribution is sensitive to the propellant formulation.

Numerical Simulation of the internal flow in the solid rocket motor and nozzle has been studied previously due to the importance of the flow field on the motor performance and reliability. The flow within the rocket is subsonic near the head end, but compressibility effects become important in the nozzle region[6)]. The flow transitions from a laminar state near the head end to a fully turbulent state farther downstream. Jayant S. Sabnis[3)] used Eulerian-Lagrangian two-phase approach suitable for the numerical simulation of the multiphase reacting internal flow in the solid rocket motor with a metalized propellant. He used an Eulerian description to analyze the motion of the gas phase particulates while Lagrangian description is used for the analysis of the discrete phase that consists of the larger particulate in the motor chamber.

To provide design guides for maintaining high performance of the SRM, an accurate simulation of the gas–particle interaction is very important. Because of the complex flow field inside the SRM, limited experiment data is available for design purpose. The internal flow field analysis using a CFD (computational fluid dynamics) method can be utilized to obtain a better investigation for SRM, due to the recent progress in computing power. There has been some research conducted in the past for the Solid Rocket Motor internal flow field analysis using the CFD method.

In this paper CFD simulation has been conducted for uniform particles size diameter to analyze its effect on the performance prediction of solid rocket motor. The Rosin-Rammler diameter distribution method and Eulerian-Lagrangian Approach[7)12)] has been used for the simulation of different distribution of $Al_2O_3$ droplets present in the motor. Because the distribution of the particles affects the performance of the motor, therefore prediction of the particles effect plays an important role for SRM design. The effect of injected droplets size distribution obtained with different models is investigated and shows the sensitivity of this distribution to the nozzle flow dynamics, primarily at the nozzle inlet and exit. The results are shown with various sizes of the particles, concentrations and geometrical configurations including models for conical and contours type nozzle, including the performance prediction.

## Model description

### Equations of Motion for Particles:

The reacting multiphase flow in the solid rocket chamber can be effectively treated as consisting of a continuous phase composed of the products of combustion from the binder, the ammonium per chlorate (AP), and reacted aluminum, and a discrete phase composed of particles containing aluminum and $Al_2O_3$. Using Eulerian-Lagrangian approach trajectories of a discrete phase particles are simulated by solving an equation of motion for each dispersed phase particle[7)]. Trajectory calculations require the calculation of net force acting on the dispersed phase particles, it will be necessary to solve a set of coupled ordinary differential equations. This force balance equates the particle inertia with the forces acting on the particle, and can be written[8)]:

$$\frac{d\overrightarrow{V_p}}{dt} = \frac{3}{4}\frac{C_d \rho}{\rho_p d_p} \| \vec{V} - \vec{V}_p \| (\vec{V} - \vec{V}_p) + \vec{g} \qquad (1)$$

Where the drag coefficient $C_d$ can be obtained:

$$C_d = \frac{24}{\mathrm{Re}_p}(1. + 0.15\,\mathrm{Re}_p^{0.687}) \qquad (2)$$

Reynolds number $Re_p$ is defined as:

$$\mathrm{Re}_p = \frac{\rho_g V_{rp} d_p}{\mu_g} \qquad (3)$$

Where $V_{rp}$ is the relative velocity between the particle velocity and the gas velocity.

### Roe scheme-FDS

Roe scheme-Flux differencing splitting (1980) based on approximate Riemann problem[9)] has been used through Fluent 6.3. This is second order upwind scheme in which flux differencing splitting method is employed. Upwind schemes are designed to numerically simulate more properly the direction of the propagation of information in a flow field along the characteristic curves. This scheme has been used with good success in computing the solution to non linear system is to solve an approximate Riemann problem rather than having to deal with the exact nonlinear iterative scheme.

The Rosin–Rammler distribution function is based on the assumption that an exponential relationship exists between the droplet diameter, d and mass fraction of droplets with diameter greater than d.

$$Y_d = e^{-(\frac{d}{\bar{d}})^n} \qquad (4)$$

Here

$\bar{d}$ = Mean Diameter of the particles
n = Spread Parameter

Particles sizes in the range of 1~100 μm are used, as being the most common droplets[10-11-12)]. In this approach the complete range of particle sizes is divided into a set of discrete size ranges, each to be defined by a single stream that is part of the group. In this case the particle size data obeys the distribution shown in Fig.2.

The table-1 below summarizes the test matrix for the various droplets diameters distributions used. For the skewed logarithmic distributions different profiles have been chosen as diagrammatical represented in Fig.2.

Table-1 Particles diameters distributions and mass fractions for different spread parameters `n

| Particles diameters distributions and mass fractions for different spread parameters `n | | | |
|---|---|---|---|
| For n = 1 | | For n = 3.5 | |
| Diameter, Range (μm) | Mass Fraction in Range | Diameter, Range (μm) | Mass Fraction in Range |
| 1.0 μm | 0.9048 | 1.0 μm | 0.9997 |
| 2.0 μm | 0.8187 | 2.0 μm | 0.9964 |
| 3.0 μm | 0.7408 | 3.0 μm | 0.9853 |
| 5.0 μm | 0.6065 | 5.0 μm | 0.9154 |
| 7.0 μm | 0.4965 | 7.0 μm | 0.7505 |
| 9.0 μm | 0.4065 | 9.0 μm | 0.5007 |
| 11.0 μm | 0.3328 | 11.0 μm | 0.2475 |
| 12.5 μm | 0.2865 | 12.5 μm | 0.1126 |
| 23.0 μm | 0.1002 | 23.0 μm | 9.7 e-9 |
| 34.0 μm | 0.0333 | 34.0 μm | 3.35 e-32 |
| 45.0 μm | 0.0111 | 45.0 μm | 1.11 e-84 |
| 56.5 μm | 0.0035 | 56.5 μm | 6.0 e-187 |
| 67.0 μm | 0.0012 | 67.0 μm | 0.0000 |
| 77.5 μm | 0.00043 | 77.5 μm | 0.0000 |
| 88.5μm | 0.00014 | 88.5 μm | 0.0000 |
| 100 μm | 0.00000 | 100 μm | 0.0000 |

## Motor and Nozzle geometry

The motor and nozzle geometry configuration adopted here is shown in the Fig.1. It represents a typical solid rocket motor with convergent and divergent nozzle. The cylindrical grain geometry with 5000 mm length of motor were tried with conical and contours nozzles. Moreover the propellant and nozzle parameters have also been dictated for all the cases.

a. Grain Length, L 5000 mm
b. Mass of propellant, $m_p$ 5500±10 kg
c. Burning time, $t_b$ 55 sec
d. Grain outer radius, R 800 mm
e. Area ratio, $A_e/A_t$ 11.7

**Parameter values and Material Selection for Discrete-phase**

Inert particle type material $Al_2O_3$ has been used. The following reference parameter values have been assumed for all the computations.

Chamber Pressure, P = 6.2 Mpa
Combustion Temperature, $T_C$ = 3200 K
Specific heat at constant Pressure, Cp = 1430 j/kg-k
Ratio of specific heats, $\gamma$ = 1.19
Density, kg/m$^3$ $\rho$ = 3910
Thermal conductivity, w/m-k = 0.1

**Boundary conditions for Discrete phase**

Following boundary conditions have been imposed on the configurations for discrete phase flow passing through the nozzle and chamber of the model.

a. A nonslip velocity is imposed for the head end, the nozzle walls, and walls at divergent part.
b. Supersonic out flow conditions are applied at the nozzle outlet.
c. For the axis, only a symmetry conditions has been applied.
d. Percentage of particles in the mass flow rate has been set.
e. 3200 K temperature is set along the bottom and top injection surfaces.
f. Pressure of 62 bars has been set inside the chamber.
g. The droplets are injected at zero velocity and are assumed to be in thermal equilibrium with the surrounding gas.

**Geometry & Computational Grid for Nozzle models being used:**

Fig.3 shows the computational domain and the grid for contours nozzle geometry. The computational grid used in these calculations consisted of 50 Grid points distributed along the radial direction and 100 grid points distributed along the motor axis. Grid resolutions near the wall were appropriate to properly resolve the flow gradient at the walls

Fig.4 shows a schematic of conical nozzle geometry. The computational grid used in these calculations consisted of 50 Grid points distributed along the radial direction and 100 grid points distributed along the nozzle axis.

## Flow field Analysis

The solution of the flow field and particle trajectories has been done using Fluent 6.3, which solve the multi-phase flow simulations and its application on performance prediction of the Solid Rocket Motor Nozzle. The flow field is solved for a chosen burn time the particle are injected from the propellant surface and tracked through, until they reach the nozzle exit and impact on the wall. Following conclusions and result are achieved.

Performance predictions for different models are tabulated in the table-2 below. A computational fluid dynamics simulation has been performed in a representative rocket motor nozzle with contour exit profile shown in Fig.3. Specific concentration has been given to nozzle flow field; however motor with the length of 5.00 m has been used. The propellant grain has 0.80 m outer diameters with propellant weight of 5500 Kg.

In model-A uniform particles distributions, the particles having one diameter size d=10 µm has been used. Mach number contours details Fig.5 and specific impulse achieved for that particular case is 1457.90 as mentioned in the table-2. In model-B two–phase flow with Rosin-Rammler diameter particles distribution with spread parameter n=1 has been used. Minimum diameter of 1e-06 m and maximum of 0.0001 m with total flow rate of 23 kg/sec has been selected. Fig.6 shows flow field for Mach number contours details, with specific impulse of 1406.46. In model-C and model-D two–phase flow with same particles diameter distribution and spread parameter n=3.5 and 10 has been used. The specific impulse of 1432 and 1395 has been achieved respectively.

The simulation presented above it is concluded that particles distributions has major role in performance prediction of the solid rocket motor. Therefore if we are more specific or close to the diameter distribution of particle with, it is giving more exact results. As from the table-2 below best performance is achieve through model-C with spread parameter n=3.5. From simulations it is also seen that particle with more diameters are moving close towards the centre or axis and lighter particles are going away from the axis Fig.9.

This paper also indicate that particle distributions has 2~3 % performance difference, so multi group is more perfect method to be applied for contour nozzle performance prediction.

The effects of uniform particles and multi-group particles on Mach numbers flow field are shown in Fig.5 & Fig.6. The Mach number is less than 0.2 at the nozzle inlet, reaches to 1.0 at the throat for both the cases. The maximum Mach number of 3.09 at the nozzle exit is reached for uniform particles and maximum of 2.85 is reached for multi-group particles. The contours are affected strongly by the particles concentration. This will affect the motor performance.

The most important effect is in the supersonic part of the nozzle. As seen through comparison till sonic line flow field for uniform particles and multi-group particles is the same but in the divergent part of it flow field simulations are different as clearly visible in the Fig.7 & Fig.8. This variation in the flow field is actually creating the difference in the performance prediction also.

Table-2 Comparisons for multi-phase flow using contours Nozzle.

| Models Description | Performance Prediction (Specific Impulse) m/sec |
|---|---|
| Model-A (Two-phase flow uniform particles distribution) | $I_{sp}$ = 1457.90 |
| Model-B (Two phase flow, spread parameter n=1) | $I_{sp}$ =1406.46 |
| Model-C (Two phase flow, spread parameter n=3.5) | $I_{sp}$ =1432.10 |
| Model-D (Two phase flow, spread parameter n=10) | $I_{sp}$ =1395.20 |

The results obtained also show a great sensitivity of particles dispersion to the size of the particles. The most dispersed particles are the smallest ones, while the larger particles almost remain towards the centre axis of the nozzle Fig.9. The small particle radius computations show that particles can be in contact with the wall even in the supersonic nozzle part.

The multiphase flow computations are also performed on nozzle with the conical divergent exit section. The same motor parameter has been used. In model-A uniform particles distributions, the particles having one diameter size d=10 µm was chosen to review, while in other models Rosin-Rammler diameter distribution method with spread parameter n=3.5 and 10 has been used. Computation has been performed on the different models with the conclusion that little difference appears in uniform particle distribution and multi–group model as clearly reported in the table-3 below. So this mean except the particle distributions nozzle divergent exit section play an important role in the performance prediction of the solid rocket motor design.

Table-3 Comparisons for two-phase flow using conical Nozzle.

| Models Descriptions | Performance Prediction (Specific Impulse) m/sec |
|---|---|
| Model-E (Two-phase flow uniform particles distribution) | $I_{sp}$ = 1379.50 |
| Model-F (Two phase flow, spread parameter n=3.5) | $I_{sp}$ =1382.56 |

| | |
|---|---|
| Model-G (Two phase flow, spread parameter n=10) | $I_{sp}$ =1391.10 |

Flow field of pressure contours for uniform particles size and multi-group phase flow are shown in the Fig.10 to Fig.13 respectively. The flow field is smooth without the effects of particles. The maximum pressure at the nozzle inlet is 5.8 Mpa and reaches to 0.42 Mpa at the nozzle exit.

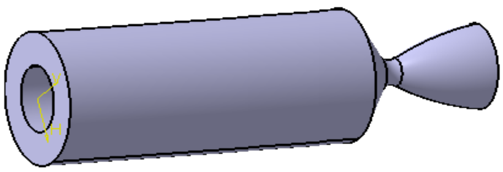

Fig. 1 Chamber, grain and Nozzle Geometry

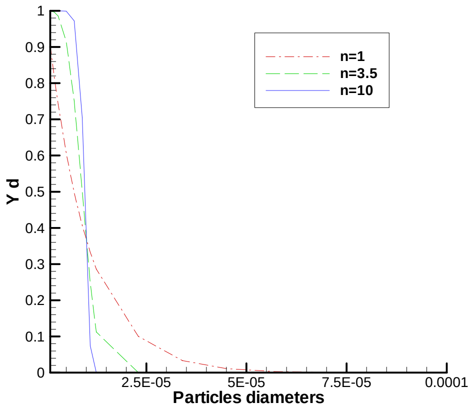


Fig.2 Value of n (n=1, 3.5, 10)

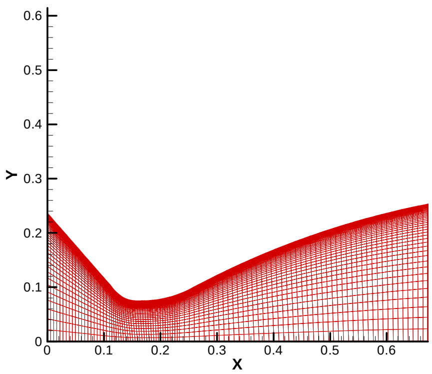


Fig.3 Grid generation for contours Nozzle

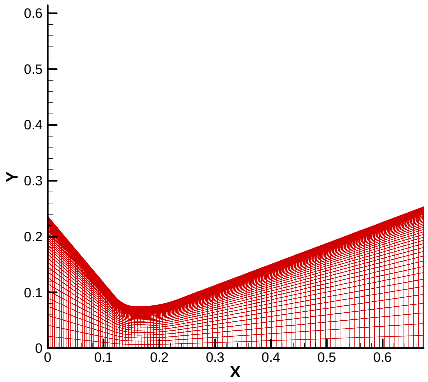


Fig.4 Grid generation for conical Nozzle

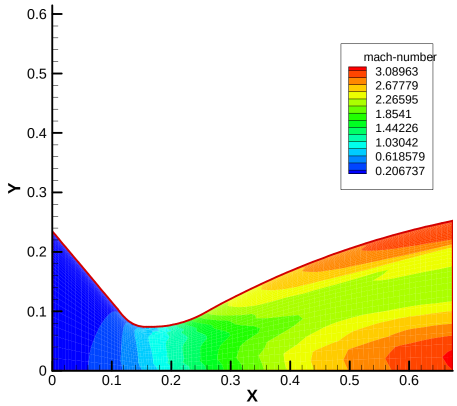


Fig.5 Mach No contours for uniform particles flow field.

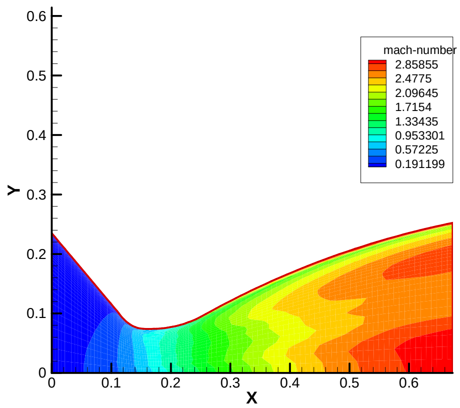


Fig.6 Mach No contours for Multi-group particles

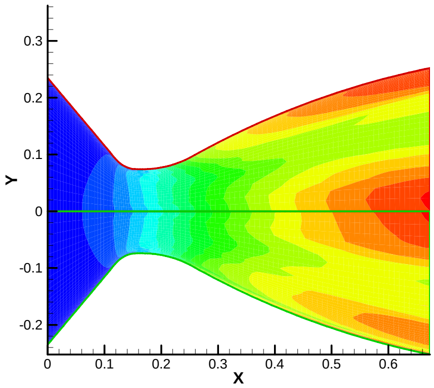


Fig.7 Comparisons of the Flow field for uniform particle & Multi-group of the particles

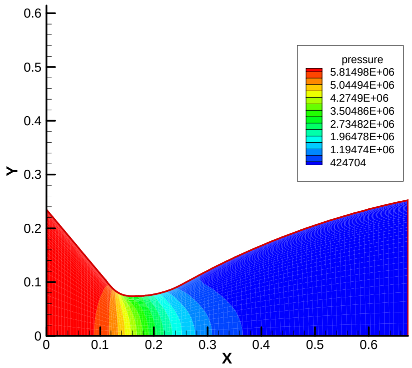


Fig.10 Pressure contours for uniform particles phase flow field.

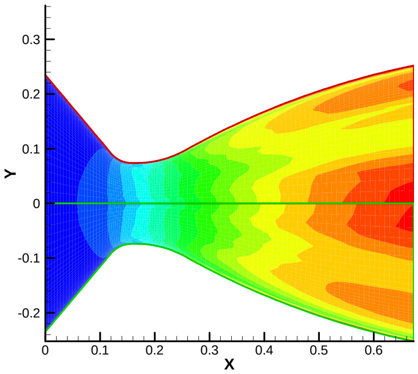


Fig.8 Comparison of Multi-particles Flow field For n=1 & n=3.5

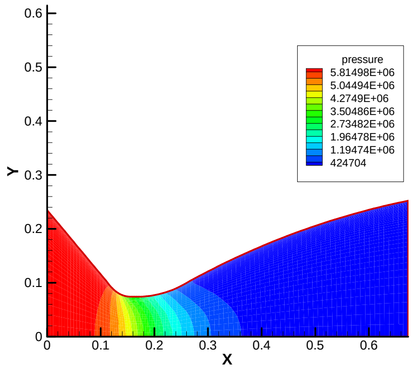


Fig.11 Pressure contours for Multi group particles

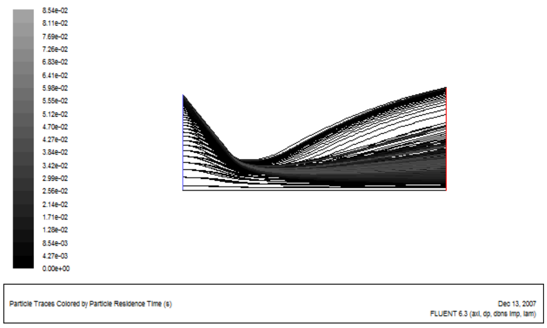

Fig.9 Particles track for Multi-group particles

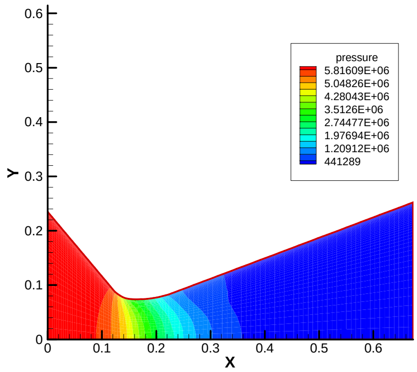


Fig.12 Pressure contours for uniform particles phase flow

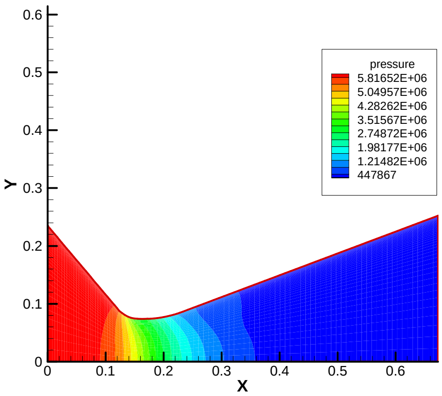


Fig.13 Pressure contours for Multi group particles

## Conclusions

Multiphase flow simulations for a typical configuration have been performed with burning aluminum droplets generating aluminum oxide. For droplet size distributions, uniform particles diameters and Rosin-Rammler diameter distribution method has been used. Roe's-FDS with Eulerian – Lagrangian approach has been applied. Two schemes one based on basic design configuration of nozzle other on the various sizes of particles with various concentrations have been used. The effects of these distributions on the flow dynamics specifically at the nozzle inlet and exit are observed.

The analysis discussed provides a more sophisticated tool for solid rocket motor internal flow field predictions. This study highlight the performance influence appears due to the diameters distribution and its particles concentrations in propellant formulation. A better performance of the solid rocket motor can also be achieved by optimizing geometric shape of nozzle, while using multi-phase flow field simulations. The results obtained can provide the designer a basic guide line for the use of materials and ultimately the design of nozzle geometry.

There are still important points that have to be further investigated to gain further insight into the multiphase flow dynamics. Future research efforts should be directed in particle distributions with more emphasis on heat transfer calculations and its impingements on the nozzle surface material that causes ablation phenomena.

## References

1) Jayant S.Sabnis.: Numerical Simulation of Distributed combustion in Solid Rocket Motors with Metalized Propellant, Journal of Propulsion and Power, Vol. 19 No 1, January-February 2003.

2) T.L.Jackson, F.Najjar, J. B uckmaster.: New Aluminum Agglomeration Model and Their Use in Solid-Propellant-Rocket Simulations, Journal of Propulsion and Power, Vol. 21 No 5, September-October 2005.

3) Sabnis,J.S.,deJong,F.J and Gibeling, H.J.: A Two-Phase Restricted Equilibrium Model for Combustion of Metalized Solid Propellant, AIAA Paper, 92-3509, July 1992.

4) Salita, M.: Quench Bomb Investigation of $Al_2$ $O_3$ formation from Solid Rocket Propellants. II Analysis of Data, 25th JANNAF Combustion Meeting, CPIA 498, Vol. 1 1988, pp.185-197.

5) Whitesides, R.H., Dill, R. A., and Purinton, D.C.: Application of Two-Phase CFD Analysis to the Evaluation of Asbestos-Free Insulation in the RSRM, IAA Paper 97-2861, July 1997.

6) F. M.Najjar, J. P. Ferry.: Simulation of Solid Propellant Rockets Effect of Aluminum Droplet Size Distribution, Journal of Propulsion and Power, Vol. 43 No 6, November-December 2006

7) Vivek V.Rande.: Comptational Flow Modeling for Chemical Rocket Engineering.

8) N.Cesco, G.Lavergne, J.L.Estivalezes.: Simulation of the Two Phase Flow in Solid Rocket Motor, AIAA-96-2640.

9) John C Tannehill Dale A.Anderson. Richard H.Pletcher.: Computational Fluid Mechanics and Heat Transfer, Second Edition.

10) E.W.Price.: Combustion of Metalized Propellants, Published in Fundamentals of Solid-Propellant Combustion, By Kenneth K.Kw & Martin Summerfield.

11) D. Desnoyer.: Two Phase Nozzle and Chamber Flow in Solid Rocket Motor, AIAA-87-0364.

12) Alessandro Ciucci, Gianluca Iaccarino, Marcello Amato.: Numerical Investigation of 3D Two-Phase Turbulent Flows in Solid Rocket Motor, AIAA-98-3966.

## APPENDIX

### Nomenclature

| | | |
|---|---|---|
| Chambers pressure | = | P |
| Grain outer radius | = | $R$ |
| Grain Length, mm | = | L |
| Mass of propellant | = | $m_p$ |
| Specific Impulse | = | $I_{sp}$ |
| Burning time | = | $t_b$ |
| Area Ratio | = | $A_e/A_t$ |
| Specific heat at constant pressure | = | $C_P$ |
| Combustion Temperature | = | $T_c$ |

| | | |
|---|---|---|
| Specific heat Ratio | = | $\gamma$ |
| Density | = | $\rho$ |
| Spread parameters | = | n |
| Mean diameter of particle | = | $\bar{d}$ |
| Molecular viscosity of the fluid | = | $\mu$ |
| Density of particle | = | $\rho_p$ |
| Particle diameter | = | $d_p$ |
| Reynolds number | = | $Re_p$ |
| Relative velocity between particles And gas velocity | = | $V_{rp}$ |